



**SLOVENSKI STANDARD**  
**kSIST-TP FprCEN/CLC/TR 17603-31-08:2021**  
**01-maj-2021**

---

**Vesoljska tehnika - Priročnik za toplotno zasnovno - 8. del: Toplotne cevi**

Space Engineering - Thermal design handbook - Part 8: Heat Pipes

Raumfahrttechnik - Handbuch für thermisches Design - Teil 8: Wärmerohre

Ingénierie spatiale - Manuel de conception thermique - Partie 8: Caloducs

**Ta slovenski standard je istoveten z: FprCEN/CLC/TR 17603-31-08**

[kSIST-TP FprCEN/CLC/TR 17603-31-08:2021](https://standards.iteh.ai/catalog/standards/sist/23b8b8d6-b049-40d7-b43e-9d8a2b04303c/ksist-tp-fprcen-clc-tr-17603-31-08-2021)

<https://standards.iteh.ai/catalog/standards/sist/23b8b8d6-b049-40d7-b43e-9d8a2b04303c/ksist-tp-fprcen-clc-tr-17603-31-08-2021>

**ICS:**

49.140 Vesoljski sistemi in operacije Space systems and operations

**kSIST-TP FprCEN/CLC/TR 17603-31-08:2021 en,fr,de**

**iTeh STANDARD PREVIEW**  
**(standards.iteh.ai)**

[kSIST-TP FprCEN/CLC/TR 17603-31-08:2021](https://standards.iteh.ai/catalog/standards/sist/23b8b8d6-b049-40d7-b43e-9d8a2b04303c/ksist-tp-fprcen-clc-tr-17603-31-08-2021)

<https://standards.iteh.ai/catalog/standards/sist/23b8b8d6-b049-40d7-b43e-9d8a2b04303c/ksist-tp-fprcen-clc-tr-17603-31-08-2021>

TECHNICAL REPORT  
RAPPORT TECHNIQUE  
TECHNISCHER BERICHT

**FINAL DRAFT**  
**FprCEN/CLC/TR 17603-31-08**

February 2021

ICS 49.140

English version

## Space Engineering - Thermal design handbook - Part 8: Heat Pipes

Ingénierie spatiale - Manuel de conception thermique -  
Partie 8: Caloducs

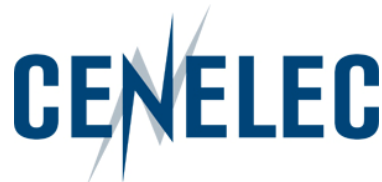
Raumfahrttechnik - Handbuch für thermisches Design -  
Teil 8: Wärmerohre

This draft Technical Report is submitted to CEN members for Vote. It has been drawn up by the Technical Committee CEN/CLC/JTC 5.

CEN and CENELEC members are the national standards bodies and national electrotechnical committees of Austria, Belgium, Bulgaria, Croatia, Cyprus, Czech Republic, Denmark, Estonia, Finland, France, Germany, Greece, Hungary, Iceland, Ireland, Italy, Latvia, Lithuania, Luxembourg, Malta, Netherlands, Norway, Poland, Portugal, Republic of North Macedonia, Romania, Serbia, Slovakia, Slovenia, Spain, Sweden, Switzerland, Turkey and United Kingdom.

Recipients of this draft are invited to submit, with their comments, notification of any relevant patent rights of which they are aware and to provide supporting documentation.

**Warning** : This document is not a Technical Report. It is distributed for review and comments. It is subject to change without notice and shall not be referred to as a Technical Report.



**CEN-CENELEC Management Centre:**  
**Rue de la Science 23, B-1040 Brussels**

## Table of contents

<b>European Foreword</b> .....	<b>10</b>
<b>1 Scope</b> .....	<b>11</b>
<b>2 References</b> .....	<b>12</b>
<b>3 Terms, definitions and symbols</b> .....	<b>13</b>
3.1 Terms and definitions .....	13
3.2 Symbols.....	13
<b>4 General introduction</b> .....	<b>17</b>
<b>5 Heat pipe wicks</b> .....	<b>19</b>
5.1 General.....	19
5.2 Basic properties.....	20
5.2.1 Equilibrium capillary height.....	20
5.2.2 Permeability.....	20
5.2.3 Effective thermal conductivity of the wick .....	20
5.3 Low resistance wicks .....	22
<b>6 Heat pipe working fluids</b> .....	<b>28</b>
6.1 General.....	28
6.2 Empirical correlations .....	29
6.3 Physical properties .....	31
6.4 Compatibility with wicks .....	47
<b>7 Simple heat pipe</b> .....	<b>48</b>
7.1 General.....	48
7.2 Operating limits.....	48
7.2.1 Capillary heat transfer limit.....	49
7.2.2 Sonic limit (choking).....	54
7.2.3 Entrainment limit .....	56
7.2.4 Boiling limit.....	56
7.3 Performance .....	57
<b>8 Variable conductance heat pipes</b> .....	<b>70</b>

8.1	General.....	70
8.2	Design considerations .....	72
8.2.1	Diffusion of the working fluid .....	72
8.2.2	Working fluid selection .....	73
8.2.3	Reservoir sizing .....	74
<b>9</b>	<b>Existing System.....</b>	<b>78</b>
9.1	Eads Astrium .....	78
9.2	Euro Heat Pipes .....	91
9.2.1	Aluminium Heat Pipes.....	91
9.2.2	STAINLESS STEEL HEAT PIPES. This part deals with the products from Technical Data Sheet n° 1B: EHP Stainless Steel.....	101
9.3	Iberespacio.....	106
9.3.1	Axial Grooved Heat Pipes .....	106
9.3.2	Arterial Heat Pipes .....	109
9.4	Thales Alenia Space.....	111
9.4.1	Technical Description.....	111
9.4.2	External Geometries.....	113
<b>10</b>	<b>Cryogenic heat pipes .. (<a href="https://standards.iteh.ai/catalog/standards/sist/23b8b8d6-b049-40d7-b43e-9d8a2b04303c/ksist-tp-fprcen-clc-tr-17603-31-08-2021">standards.iteh.ai</a>).....</b>	<b>116</b>
10.1	General.....	116
10.2	Working fluids.....	116
10.3	Wicks.....	118
10.3.1	Lab wicks .....	120
10.3.2	Tunnel artery.....	120
10.3.3	Graded-porosity wicks.....	120
10.4	Operating limits.....	121
10.4.1	Capillary heat transfer limit.....	121
10.5	Transient operating characteristics .....	127
10.5.1	Mathematical modelling of static transient.....	127
10.5.2	Mathematical modelling of fluid dynamic transient.....	128
10.6	Reduced gravity testing of cryogenic heat pipes .....	129
10.7	Thermal diode cryogenic heat pipes .....	131
10.7.2	Reversal requirements .....	132
10.8	Superfluid heat pipes .....	134
10.9	Existing systems .....	138
	<b>Bibliography.....</b>	<b>146</b>

## FprCEN/CLC/TR 17603-31-08:2021 (E)

## Figures

Figure 5-1: Measured values of the inverse permeability, $K^{-1}$ , vs. mass flow rate per unit area, $\dot{m}$ . > From Phillips & Hinderman (1969) [67].	27
Figure 5-2: Measured values of the inverse permeability, $K^{-1}$ , vs. mass flow rate per unit area, $\dot{m}$ . > From Phillips & Hinderman (1969) [67].	27
Figure 6-1: Relevant physical properties of Ammonia as a function of temperature, $T$ , The labels correspond to experimental points. The expressions used to calculate the tabulated values are given below. Calculated by the compiler.	32
Figure 6-2: Relevant physical properties of Ethanol as a function of temperature, $T$ , The labels correspond to experimental points. The expressions used to calculate the tabulated values are given below. Calculated by the compiler.	34
Figure 6-3: Relevant physical properties of Freon 11 as a function of temperature, $T$ , The labels correspond to experimental points. The expressions used to calculate the tabulated values are given below. Calculated by the compiler.	36
Figure 6-4: Formulae Used for Calculating the Values of the Physical Properties.	38
Figure 6-5: Relevant physical properties of Nitrogen as a function of temperature, $T$ , The labels correspond to experimental points. The expressions used to calculate the tabulated values are given below. Calculated by the compiler.	40
Figure 6-6: Relevant physical properties of Propane as a function of temperature, $T$ , The labels correspond to experimental points. The expressions used to calculate the tabulated values are given below. Calculated by the compiler.	42
Figure 6-7: Relevant physical properties of Water as a function of temperature, $T$ , The labels have been drawn to guide in the selection of the appropriate curve, and do not correspond to experimental values. After Schmidt (1969) [82].	44
Figure 6-8: Figure of Merit, $N$ , as a function of temperature, $T$ , for several heat pipe working fluids. For each curve, the range of temperature variation is bounded between the largest and smallest operating pressures. Calculated by the compiler.	46
Figure 7-1: Sketch illustrating design variables in grooved heat pipes. From Frank et al. (1967) [27], quoted by Winter & Barsch (1971) [96].	51
Figure 7-2: Relation between the dimensionless parameter $16/\beta(v_w/v_l)F$ and the geometrical parameter, $\psi$ . From Frank et al. (1967) [27], quoted by Winter & Barsch (1971) [96].	52
Figure 7-3: Optimum value of the dimensionless maximum heat transfer, $Q_{max}/Tr_w^3$ , vs. the geometrical parameter, $\psi$ . From Frank et al. (1967) [27], quoted by Winter & Barsch (1971) [96].	53
Figure 7-4: Graph for determining $F$ . From Frank et al. (1967) [27], quoted by Winter & Barsch (1971) [96].	53
Figure 7-5: Optimum value of the aspect ratio of the grooves, $\alpha$ , vs. the geometrical parameter, $\psi$ . From Frank et al. (1967) [27], quoted by Winter & Barsch (1971) [96].	54
Figure 7-6: Maximum heat transfer, $Q_{max}$ , based on sonic limit, vs. evaporator temperature, $T_E$ , for several values of the shear stresses, $\tau$ , and of the convective heat transfer, $Q_{conv}$ . Sodium heat pipe. A: $\tau = 0$ and $Q_{conv} = 0$ ; B: $\tau \neq 0$ and $Q_{conv} \neq 0$ ; C: $\tau \neq 0$ and $Q_{conv} = 0$ ; D: $\tau = 0$ and $Q_{conv} \neq 0$ . In this case the heat pipe had an adiabatic length. In curves A, B, and C choking is	

reached at the evaporator, while in curve D choking is reached at the adiabatic length end. From Levy (1972) [49].	55
Figure 7-7: Heat Transfer, $Q_{max}$ , and Integral Heat Transport Factor, $[Q \cdot l_{eff}]_{max}$ , vs. wick thickness, $\delta$ , for several mesh sizes and two heat pipe diameters, $D_o$ . Circumferential screen wick. Solid lines: vapour laminar flow; dotted lines: vapour turbulent flow. From Skrabek (1972) [88].	58
Figure 7-8: Heat Transfer, $Q_{max}$ , and Integral Heat Transport Factor, $[Q \cdot l_{eff}]_{max}$ , vs. wick thickness, $\delta$ , for several mesh sizes and two heat pipe diameters, $D_o$ . Circumferential screen wick. Solid lines: vapour laminar flow; dotted lines: vapour turbulent flow. From Skrabek (1972) [88].	59
Figure 7-9: Heat Transfer, $Q_{max}$ , and Integral Heat Transport Factor, $[Q \cdot l_{eff}]_{max}$ , vs. wick thickness, $\delta$ , for several mesh sizes and two heat pipe diameters, $D_o$ . Circumferential screen wick. Solid lines: vapour laminar flow; dotted lines: vapour turbulent flow. From Skrabek (1972) [88].	60
Figure 7-10: Heat Transfer, $Q_{max}$ , and Integral Heat Transport Factor, $[Q \cdot l_{eff}]_{max}$ , vs. wick thickness, $\delta$ , for several mesh sizes and two heat pipe diameters, $D_o$ . Porous slab wick. Solid lines: vapour laminar flow; dotted lines: vapour turbulent flow. From Skrabek (1972) [88].	61
Figure 7-11: Heat Transfer, $Q_{max}$ , and Integral Heat Transport Factor, $[Q \cdot l_{eff}]_{max}$ , vs. wick thickness, $\delta$ , for several mesh sizes and two heat pipe diameters, $D_o$ . Porous slab wick. Solid lines: vapour laminar flow; dotted lines: vapour turbulent flow. From Skrabek (1972) [88].	62
Figure 7-12: Heat Transfer, $Q_{max}$ , and Integral Heat Transport Factor, $[Q \cdot l_{eff}]_{max}$ , vs. wick thickness, $\delta$ , for several mesh sizes and two heat pipe diameters, $D_o$ . Porous slab wick. Solid lines: vapour laminar flow; dotted lines: vapour turbulent flow. From Skrabek (1972) [88].	63
Figure 7-13: Heat pipe conductance, $C$ , vs. wick thickness, $\delta$ , for several wick conductivities, $k_{eff}$ , and two heat pipe diameters, $D_o$ . Circumferential screen wick. From Skrabek (1972) [88].	64
Figure 7-14: Heat pipe conductance, $C$ , vs. wick thickness, $\delta$ , for several wick conductivities, $k_{eff}$ , and two heat pipe diameters, $D_o$ . Circumferential screen wick. From Skrabek (1972) [88].	65
Figure 7-15: Heat pipe conductance, $C$ , vs. wick thickness, $\delta$ , for several wick conductivities, $k_{eff}$ , and two heat pipe diameters, $D_o$ . Circumferential screen wick. From Skrabek (1972) [88].	66
Figure 7-16: Heat pipe conductance, $C$ , vs. wick thickness, $\delta$ , for several values of the heat transfer coefficient of the wick, $h$ , and heat pipe diameters, $D_o$ . Porous slab wick. From Skrabek (1972) [88].	67
Figure 7-17: Heat pipe conductance, $C$ , vs. wick thickness, $\delta$ , for several values of the heat transfer coefficient of the wick, $h$ , and heat pipe diameters, $D_o$ . Porous slab wick. From Skrabek (1972) [88].	68
Figure 7-18: Heat pipe conductance, $C$ , vs. wick thickness, $\delta$ , for several values of the heat transfer coefficient of the wick, $h$ , and heat pipe diameters, $D_o$ . Porous slab wick. From Skrabek (1972) [88].	69
Figure 8-1: VCHP with cold reservoir.	71
Figure 8-2: VCHP with hot reservoir. (a) Internal hot reservoir. (b) External hot reservoir.	72

**FprCEN/CLC/TR 17603-31-08:2021 (E)**

Figure 8-3: Vapor concentration at the reservoir, $n(t)$ , over its steady-state value, $n(\infty)$ , and control temperature range, $\Delta T$ , as functions of time, $t$ . From Hinderman. Waters & Kaser (1972) [35].....	73
Figure 8-4: Dimensionless pressure ratio, $\pi_r$ , vs. control temperature range, $T_{Emax}-T_{Emin}$ , for several working fluids. From Hinderman, Waters & Kaser (1972) [35].....	74
Figure 8-5: Sketch of a variable conductance heat pipe. 1: Evaporator. 2: Adiabatic Section. 3: Condenser. 4: Adiabatic Section. 5: Reservoir.....	75
Figure 8-6: Dimensionless reservoir to condenser volume ratio, $V_R/V_C$ , vs. evaporator temperature variation, $(T_{Emax}-T_{Emin})$ , for two different working fluids, and a given reservoir temperature variation, $(T_{Rmax}-T_{Rmin}) = 28$ K. From Edelstein & Hembach (1972) [23]. .....	75
Figure 8-7: Dimensionless reservoir to condenser volume ratio, $V_R/V_C$ , vs. reservoir temperature variation, $(T_{Rmax}-T_{Rmin})$ , with fixed evaporator control temperature variation, $(T_{Emax}-T_{Emin}) = 6$ K. From Edelstein & Hembach (1972) [23].....	76
Figure 8-8: Dimensionless reservoir to condenser volume ratio, $V_R/V_C$ , vs. evaporator temperature variation, $(T_{Emax}-T_{Emin})$ , for ammonia working fluid. From Edelstein & Hembach (1972) [23].....	76
Figure 8-9: Dimensionless reservoir to condenser volume ratio, $V_R/V_C$ , vs. evaporator temperature variation, $(T_{Emax}-T_{Emin})$ . Solid lines: cold reservoir. Dashed lines: hot reservoir. (A) and (M) correspond to ammonia and methanol respectively. $T_s$ is the sink temperature; in one case the back of the radiator is painted black ( $222 \text{ K} < T_s < 254 \text{ K}$ ), and in the other it is aluminized ( $196 \text{ K} < T_s < 245 \text{ K}$ ). Evaporator temperature, $T_E = (287 + (T_{Emax}-T_{Emin})/2)$ K. From Kirkpatrick & Marcus (1972) [42].....	77
Figure 9-1: WR7 Heat Pipe Profile (Cryogenic Application).....	83
Figure 9-2: WR12 Heat Pipe Profile.....	84
Figure 9-3: WR18 Heat Pipe Profile.....	84
Figure 9-4: WR19 Heat Pipe Profile.....	85
Figure 9-5: WR20 Heat Pipe Profile.....	85
Figure 9-6: WR22 Heat Pipe Profile.....	86
Figure 9-7: WR24 Heat Pipe Profile.....	86
Figure 9-8: WR25 Heat Pipe Profile.....	87
Figure 9-9: WR26 Heat Pipe Profile.....	87
Figure 9-10: WR27 Heat Pipe Profile.....	88
Figure 9-11: WR28 Heat Pipe Profile.....	88
Figure 9-12: WR29 Heat Pipe Profile.....	89
Figure 9-13: WR7 Heat Pipe used for SCIAMACHY on ENVISAT.....	89
Figure 9-14: EADS ASTRIUM HP experience.....	90
Figure 9-15: EHP: typical Aluminium extruded HP.....	91
Figure 9-16: Heat transport capability – NH3 (Note: AG110 = size 11 mm in tens of millimetres.).....	94
Figure 9-17: HP Profile Tolerances.....	97



Figure 9-18: HP Profile Tolerances (cont.).....	98
Figure 9-19: HP Profile Tolerances (cont.).....	99
Figure 9-20: ESA SMART 1 with HP .....	100
Figure 9-21: ESA AEOLUS – ALADIN instrument with HP network.....	100
Figure 9-22: Constant Conductance Heat Pipe .....	101
Figure 9-23: Variable Conductance Heat Pipe.....	101
Figure 9-24: Heat Pipe Profiles examples Table 9.2-3. Stainless Steel Heat Pipes types. ....	102
Figure 9-25: “Thank to 40 state-of-the art variable conductance heat pipes located in the avionics bay the ATV is able to carry away the heat and release the energy directly into space or, otherwise, to warm up other parts in a very economic fashion” Astrium – ESA “Jules Verne goes hot and cold” – Successful achievement of the Qualification Thermal Test campaign – 14 Dec 2006.....	104
Figure 9-26: Stainless Steel HP Performance curves .....	105
Figure 9-27: Stainless Steel HP Performance curves (cont.) .....	105
Figure 9-28: Axial Grooved HP profiles .....	106
Figure 9-29: Axial Grooved HP profiles drawings .....	107
Figure 9-30: Dependence of AGHP Heat Transfer Capacity on Working Fluid (Ammonia) .....	108
Figure 9-31: Influence of tilt angle on AGHP maximum Heat Transfer Capacity at 20°C ....	108
Figure 9-32: Thermal performance of Arterial HP with different working fluids.....	109
Figure 9-33: Experimental data for Arterial HP with ammonia.....	109
Figure 9-34: Arterial HP profile schematics.....	110
Figure 9-35: Arterial HP typical configurations.....	110
Figure 9-36: Arterial HP for rotator application. Length 2400 mm. Power 150 W. ....	111
Figure 9-37: 0g guaranteed heat transport capability for ThalesAlenia Space Heat Pipes.....	112
Figure 9-38: Mono-core heat pipe profile.....	113
Figure 9-39: Dual-core heat pipe profiles.....	114
Figure 9-40: Minimal dimensions of straight parts for Ø 12.2 bent heat pipe.....	115
Figure 10-1: Operating temperature range for cryogenic working fluids. Data from ECSS-E-HB-31-01 Part 14, Table 8-1, clause 8.1.1. For fluorine: melting point, $T = 53,5$ K, critical point, $T = 144$ K.....	117
Figure 10-2: Figure of Merit, $N$ , as a function of temperature, $T$ , for several cryogenic working fluids. Compare with Figure 6-8, clause 6.3. Replotted after Chi & Cygnarowicz (1970) [15]. ....	118
Figure 10-3: Axial distribution of porosity, $\Phi$ , and cross section of a graded-porosity slab wick. From Groll, Pittman & Eninger (1976) [30]. ....	121
Figure 10-4: Maximum heat transport factor, $(Q \cdot l_{eff})$ , for a homogeneous wick heat pipe as a function of inner diameter, $D_i$ , for different gravity levels. a) Working fluid is Nitrogen at 77 K. b) Oxygen at 77 K. From Joy (1970) [38]. ....	124

**FprCEN/CLC/TR 17603-31-08:2021 (E)**

Figure 10-5: Maximum heat transport factor, $(Q./I_{eff})$ , for an axially grooved heat pipe and for a homogeneous wick heat pipe vs. inner diameter of the pipe, $D_i$ , for different gravity levels. Working fluid is Oxygen at 77 K. From Joy (1970) [38].....	125
Figure 10-6: Axial temperature drop, $\Delta T$ , for Oxygen heat pipes at 77 K vs. inner diameter of the pipe, $D_i$ . Also shown are data for an axially grooved heat pipe and for aluminium rods of the same diameter. From Joy (1970) [38]. Calculation procedure is outlined in the text. ....	126
Figure 10-7: Nodal points in the static transient model of a heat pipe. From Smirnov, Barsookov & Mishchenko (1976) [89].....	127
Figure 10-8: Schematic of the heat pipe considered by Chang & Colwell (1985) [13]. ....	128
Figure 10-9: ERTS-C (Landsat III) cryogenic heat pipe experiment configuration. From Brennan & Kroliczek (1975) [45].....	130
Figure 10-10: Schematic of a blocking orifice thermal diode heat pipe. From Kosson, Quadrini & Kirckpatrick (1974) [44].....	131
Figure 10-11: a) Axial temperature profiles during reverse mode tests of a cryogenic heat pipe diode. No tilt. Tests performed in an insulated LN <sub>2</sub> cooled enclosure. At time 0 power (3 W) is removed from the evaporator, and the reservoir heater is on. $T_o$ is the ambient temperature within the enclosure. b) Shut-down temperature response of evaporator and upstream end of blocked transport section. From Quadrini & McCreight (1977) [66].....	133
Figure 10-12: Axial temperature profiles during reverse mode tests. Tests performed as in Figure 10-11a except 1 W heat load on the evaporator continuously fed during the run. $T_o$ is the ambient temperature within the enclosure. From Quadrini & McCreight (1977) [66]. ....	134
Figure 10-13: Cross section of Heat Pipe 2. From Murakami & Kaido (1980) [61]. All the dimensions are in mm. ....	135
Figure 10-14: Temperature, $T$ , vs. heat transfer rate, $Q$ , in Heat Pipe 3. $T_1$ is the evaporator temperature, $T_2$ and $T_3$ are in the adiabatic clause $88 \times 10^{-3}$ m and $78 \times 10^{-3}$ m from the evaporator end. The sink temperature is $T_s = 1,9$ K. From Murakami (1982) [60].....	136
Figure 10-15: Critical heat transfer rate, $Q_c$ , and I-transition heat transfer rate, $Q_{\lambda_s}$ , for the three heat pipes as a function of sink temperature, $T_s$ . From Murakami (1982) [60]. Key is given below. ....	137
Figure 10-16: Integral heat transport factor, $(Q./I_{eff})_{max}$ , vs. operating temperature, $T$ , of the cryogenic heat pipes tabulated in Table 10-4. ....	145

**Tables**

Table 5-1: Empirical Correlations for the Determination of Wick Properties .....	21
Table 5-2: Properties of Wick Materials .....	23
Table 6-1: Chemical Compatibility between Typical Wick Materials and Working Fluids.....	47
Table 7-1: Combinations of Temperatures, Working Fluids, Wick and Container Materials, and Heat Pipe Outer Diameters. ....	57
Table 9-1: Selected Aluminium Heat Pipe Profiles.....	79
Table 9-2: Aluminium Heat Pipe Profiles (cont.) .....	80

Table 9-3: Aluminium Heat Pipe Profiles (cont.) .....	81
Table 9-4: Aluminium Heat Pipe Profiles (cont.) .....	82
Table 9-5: Aluminium Heat Pipe Profiles (cont.) .....	83
Table 9-6: EHP Aluminium Heat Pipes Performance .....	92
Table 9-7: Available HP Profiles .....	95
Table 9-8: Stainless Steel Heat Pipes types .....	102
Table 9-9: Geometrical Parameters .....	107
Table 9-10: Thermal Performances of ThalesAlenia Space Heat Pipes (*): $QL_{max}$ 6mm guaranteed .....	112
Table 9-11: Mass of ThalesAlenia Space Heat Pipes .....	113
Table 9-12: External geometries of ThalesAlenia Space Heat Pipes .....	114
Table 10-1: Main Features of Cryogenic Fluids in Heat Pipes, Consequences .....	116
Table 10-2: Wicking Structures. Current Technology .....	118
Table 10-3: Evolution of Vapor to Liquid Kinematic Viscosity Ratio over Working Temperature Range <sup>a</sup> .....	123
Table 10-4: Characteristics of Tested Cryogenic Heat Pipes .....	138
Table 10-5: Characteristics of Tested Cryogenic Heat Pipes, Materials .....	140
Table 10-6: Characteristics of Tested Cryogenic Heat Pipes, Operating Conditions .....	142

**(standards.iteh.ai)**

[kSIST-TP FprCEN/CLC/TR 17603-31-08:2021](https://standards.iteh.ai/catalog/standards/sist/23b8b8d6-b049-40d7-b43e-9d8a2b04303c/ksist-tp-fprcen-clc-tr-17603-31-08-2021)

<https://standards.iteh.ai/catalog/standards/sist/23b8b8d6-b049-40d7-b43e-9d8a2b04303c/ksist-tp-fprcen-clc-tr-17603-31-08-2021>

## European Foreword

---

This document (FprCEN/CLC/TR 17603-31-08:2021) has been prepared by Technical Committee CEN/CLC/JTC 5 "Space", the secretariat of which is held by DIN.

This document is currently submitted to the Vote on TR.

It is highlighted that this technical report does not contain any requirement but only collection of data or descriptions and guidelines about how to organize and perform the work in support of EN 16603-31.

This Technical report (FprCEN/CLC/TR 17603-31-08:2021) originates from ECSS-E-HB-31-01 Part 8A.

Attention is drawn to the possibility that some of the elements of this document may be the subject of patent rights. CEN [and/or CENELEC] shall not be held responsible for identifying any or all such patent rights.

This document has been prepared under a mandate given to CEN by the European Commission and the European Free Trade Association.

This document has been developed to cover specifically space systems and has therefore precedence over any TR covering the same scope but with a wider domain of applicability (e.g.: aerospace).

**This document is currently submitted to the CEN CONSULTATION.**

# 1 Scope

Heat pipes are a solution to many thermal dissipation problems encountered in space systems.

The types of heat pipes that can be used in spacecrafts are described. Details on design and construction, usability, compatibility and the limitations of each type are given.

The Thermal design handbook is published in 16 Parts

TR 17603-31-01	Thermal design handbook – Part 1: View factors
TR 17603-31-02	Thermal design handbook – Part 2: Holes, Grooves and Cavities
TR 17603-31-03	Thermal design handbook – Part 3: Spacecraft Surface Temperature
TR 17603-31-04	Thermal design handbook – Part 4: Conductive Heat Transfer
TR 17603-31-05	Thermal design handbook – Part 5: Structural Materials: Metallic and Composite
TR 17603-31-06	Thermal design handbook – Part 6: Thermal Control Surfaces
TR 17603-31-07	Thermal design handbook – Part 7: Insulations
TR 17603-31-08	Thermal design handbook – Part 8: Heat Pipes
TR 17603-31-09	Thermal design handbook – Part 9: Radiators
TR 17603-31-10	Thermal design handbook – Part 10: Phase – Change Capacitors
TR 17603-31-11	Thermal design handbook – Part 11: Electrical Heating
TR 17603-31-12	Thermal design handbook – Part 12: Louvers
TR 17603-31-13	Thermal design handbook – Part 13: Fluid Loops
TR 17603-31-14	Thermal design handbook – Part 14: Cryogenic Cooling
TR 17603-31-15	Thermal design handbook – Part 15: Existing Satellites
TR 17603-31-16	Thermal design handbook – Part 16: Thermal Protection System

## 2 References

---

EN Reference	Reference in text	Title
EN 16603-00-01	ECSS-S-ST-00-01	ECSS System - Glossary of terms
TR 17603-31-10	ECSS-E-HB-31-01 Part 10	Thermal design handbook – Part 10: Phase-Change Capacitors
TR 17603-31-13	ECSS-E-HB-31-01 Part 13	Thermal design handbook – Part 13: Fluid Loops
TR 17603-31-14	ECSS-E-HB-31-01 Part 14	Thermal design handbook – Part 14: Cryogenic Cooling

**iTeh STANDARD PREVIEW**

(standards.itech.ai)

All other references made to publications in this Part are listed, alphabetically, in the **Bibliography**.

[kSIST-TP FprCEN/CLC/TR 17603-31-08:2021](https://standards.itech.ai/catalog/standards/sist/23b8b8d6-b049-40d7-b43e-9d8a2b04303c/ksist-tp-fprcen-clc-tr-17603-31-08-2021)  
<https://standards.itech.ai/catalog/standards/sist/23b8b8d6-b049-40d7-b43e-9d8a2b04303c/ksist-tp-fprcen-clc-tr-17603-31-08-2021>

## Terms, definitions and symbols

---

### 3.1 Terms and definitions

For the purpose of this Standard, the terms and definitions given in ECSS-S-ST-00-01 apply.

### 3.2 Symbols

$A_v$	vapour core cross-sectional area, [m <sup>2</sup> ]
$A_w$	wick cross-sectional area, [m <sup>2</sup> ].
$C$	heat pipe thermal conductance, [W.K <sup>-1</sup> ]
$C_i$	heat capacity associated to node $i$ , [J.K <sup>-1</sup> ]
$D_i$	inner wall diameter of the pipe, [m]
$D_o$	outer wall diameter of the pipe, [m]
$D_p$	diameter of particles, [m]
$D_v$	diameter of the vapour space, [m]
$H$	equilibrium capillary height, [m]
$H_{ij}$	heat transfer coefficient between nodes $i$ and $j$ , [W.K <sup>-1</sup> ]
$K$	permeability, [m <sup>2</sup> ]
$M$	molar mass, [kg.mol <sup>-1</sup> ]
$N$	figure of merit, [W.m <sup>2</sup> ] $N = \rho_l h_{fg} \sigma / \mu_l$
$Q$	heat transfer rate, [W]
$(Q.l_{eff})$	integral heat transport factor, [W.m]
$R$	universal gas constant, $R = 8,3143 \text{ J.K}^{-1}.\text{mol}^{-1}$
$R_g$	gas constant of a particular gas, [J.K <sup>-1</sup> .kg <sup>-1</sup> ] $R_g = R/M$
$Re$	Reynolds number, $Re = \rho V D_i / \mu$